

Direct Electrochemistry of Hemoglobin on Electrodeposited Three-Dimensional Interconnected Graphene-Silver Nanocomposite Modified Electrode

Hailiang Sha¹, Wen Zheng², Fan Shi², Xiaofeng Wang^{3,*}, Wei Sun^{2,*}

¹ School of Dentistry, Capital Medical University, Beijing 100050, P. R. China;

² College of Chemistry and Chemical Engineering, Hainan Normal University, Haikou 571158, P. R. China.

³ Department of Precision Instruments, Tsinghua University, Beijing 100084, P. R. China;

*E-mail: xfw@mail.tsinghua.edu.cn, swyy26@hotmail.com

Received: 26 June 2016 / *Accepted:* 30 August 2016 / *Published:* 10 October 2016

A three-dimensional electroreduced graphene oxide (3DGR) and silver (Ag) nanocomposite was fabricated by electrodeposition directly on the electrode surface for modification. N-butylpyridinium hexafluorophosphate (BPPF₆) was used to prepare a carbon ionic liquid electrode (CILE) and acted as the basic working electrode. Hemoglobin (Hb) was further casted on the surface of Ag/3DGR/CILE to result a bioelectrode. Direct electrochemistry of Hb on the modified electrode was accelerated with a pair of well shape redox waves on cyclic voltammogram, showing the realization of direct electron transfer. The presence of high conductive Ag/3DGR composite on the electrode facilitated the electron transfer rate from the electroactive center of Hb to the electrode. Electrochemical behaviors of Hb on the modified electrode were checked and the electrochemical parameters were calculated.

Keywords: Three-dimensional electroreduced graphene oxide, Silver nanostructure, Hemoglobin, Direct electron transfer, Carbon ionic liquid electrode.

1. INTRODUCTION

Direct electrochemistry of enzymes and redox proteins is of great importance in study on the intrinsic electrochemical properties of proteins and the results can be used for fabricating bioreactors and biosensors [1, 2]. In general the electroactive centers of redox enzymes are deeply buried within biological macromolecules, therefore direct electron transfer from the electrochemical active center of redox proteins to the substrate electrode is difficult to occur [3]. Many works have been reported to

enhance the electron transfer properties of redox proteins with different mediators, promoters or nanostructured materials, which can change the interface chemistry of the working electrode [4,5].

As one of the typical representatives of heme based proteins, hemoglobin (Hb) is well-known for its structure and functions in the vascular system, which can transport oxygen from lungs or gills to the peripheral tissues [6]. Hb is consisted of four polypeptide subunits including two α and two β subunits with a molar mass of $67,000 \text{ g mol}^{-1}$ [7], which can be commercial purchased with excellent stability. Therefore Hb is an commonly used ideal model molecule to investigate direct electron transfer of redox enzymes/proteins [8, 9]. However, on conventional solid electrodes a fast electron transfer between Hb and the electrode is impossible to be realized because of the deeply buried of the active center of Hb in polypeptide chain structures [10]. Various efforts have been designed to explore different immobilization procedures and modifiers to fast the electron transfer efficiency with the bioactivity of enzyme maintained. In recent years nanomaterials-facilitated electrochemistry of redox enzymes/proteins at electrode surfaces has aroused specific interests. Nanomaterials exhibit the properties including certain conductivity, unique catalytic properties, high amount of biocatalyst loading, excellent thermal and chemical stability, perfect adsorption and penetrability. The applications of nanomaterials in the protein electrochemistry have been widely reported [11].

Nanostructured metal material is one of the best nanomaterial for constructing electrochemical biosensor because of its good conductivity, certain catalytic ability, large surface area and good biocompatibility. Commonly used metal nanomaterials include gold, silver, platinum and other precious metals of nanoscale. Among them silver nanoparticles (AgNPs) exhibit high conductivity with good biocompatibility, which have been applied in the fields such as bioelectrocatalysis, medical diagnosis and biomedical treatment [12].

Graphene (GR) is composed of monolayer carbon atoms that packed in a two-dimensional (2D) honeycomb lattice [13]. Due to high electrical conductivity, big surface area and interlayer structures, GR is benefit for the construction of electrochemical devices. Recently three-dimensional (3D) GR has aroused great interests due to its macrostructure, which is synthesized from 2D GR nanosheets. Being a hierarchical porous macromaterial, 3D GR owns many specific performances including big surface area, highly conductive pathway, lower resistance and enhanced mobility of charge carries [14]. The ideally interconnected 3D macrostructure network is suitable for electrons to transfer easily with high efficiency. Also the analyte can be adsorbed inside the 3D structure and fully interacted with GR interface, which is suitable for the electrochemical applications [15].

Here a 3D GR and Ag nanocomposite was electrodeposited in turn onto the surface of substrate electrode, which was prepared with ionic liquid (IL) N-butylpyridinium hexafluorophosphate (BPPF₆) modified carbon paste electrode (CPE). IL modified CPE, also named as carbon ionic liquid electrode (CILE), is often used as the substrate electrode recently, which shows high performances including fast conductivity, wide electrochemical window and certain electrocatalytic capability [16]. Then Hb and chitosan (CS) were casted on Ag/3DGR/CILE to obtain a CS/Hb/Ag/3DGR/CILE. Direct electrochemistry of Hb was investigated in detail with a pair of well shaped and nearly symmetrical redox waves observed on cyclic voltammogram, indicating the realization of direct electron transfer from the electroactive centers of Hb to the electrode. Therefore the presence of Ag/3DGR nanocomposite on the electrode surface could enhance the transfer of electron.

2. EXPERIMENTAL

2.1. Reagents

Hb (MW. 64500) and silver nitrate (AgNO_3) were purchased from Sinopharm Chem. Reagent Co., China. BPPF_6 (Lanzhou Yulu Fine Chem. Co., China), graphite powder (particle size 30 μm , Shanghai Colloid Chem. Co., China), CS (Dalian Xindie Ltd. Co., China), graphene oxide (GO, Taiyuan Tanmei Co., China), lithium perchlorate (LiClO_4 , Chengdu Kelong Chem. Reagent Co., China) were used as received. 0.1 mol L^{-1} phosphate buffer solutions (PBS, different pH values) were used as the supporting electrolyte. Other chemicals were of analytical reagent grade with doubly distilled water used in the experiments.

2.2. Apparatus

Electrochemical experiments such as cyclic voltammetry and electrochemical impedance spectroscopy (EIS) were carried out with a CHI 660D electrochemical workstation (Shanghai Chenhua Instrument, China). Three-electrode system was selected with a Hb modified working electrode, a platinum wire auxiliary electrode and a saturated calomel reference electrode (SCE). Scanning electron microscopy (SEM) was recorded on a JSM-7100F scanning electron microscope (Japan Electron Company, Japan).

2.3. Preparation of the modified electrode

CILE was prepared according to the reported experimental method [16] with BPPF_6 as the modifier, which was acted as the substrate electrode for further decoration. Then 3DGR was directly formed on CILE with a potentiostatic method [17] based on the electroreduction of GO. Briefly, CILE was putted in a 1.0 mg mL^{-1} GO and 0.1 mol L^{-1} LiClO_4 mixture solution, which was treated by magnetic stirring and N_2 bubbling. Then electrochemical reduction was set at the potential of -1.3 V with the time of 300 s to get the 3DGR/CILE. After rinsed with water and dried in N_2 atmosphere, electrodeposition of Ag nanoparticles on 3DGR/CILE was further carried out in a mixture solution of 5.0 mmol L^{-1} AgNO_3 and 0.5 mol L^{-1} KNO_3 with the potential of -0.7 V for 30 s without stirring. The formed Ag/3DGR/CILE was washed with water thoroughly and dried in N_2 atmosphere. Hb modified electrode was further fabricated by casting 8.0 μL 15.0 mg mL^{-1} Hb solution directly onto Ag/3DGR/CILE. After the solution was evaporated in the air at room temperature, 5.0 μL 1.0 mg mL^{-1} CS solution (in 1.0% HAc) was casted on Hb/Ag/3DGR/CILE and the solution was evaporated to obtain the Hb modified electrode, which was put in a 4 °C refrigerator before use. Other kinds of modified electrodes such as CS/CILE, CS/3DGR/CILE, CS/Hb/CILE, CS/Hb/Ag/CILE etc. were also prepared with the similar method and used for comparison.

2.4. Electrochemical measurements

Cyclic voltammetric experiments were done at room temperature and the buffer solutions were degassed with high pure N_2 for 30 min before experiments. N_2 was remained in the electrochemical

cell during the measurements. Then three-electrode system was immersed in a 10 mL cell with 0.1 mol L⁻¹ pH 3.0 PBS and cyclic voltammograms were recorded in the potential windows from 0.2 to -0.6 V (vs. SCE) with scan rate as 100 mV s⁻¹. EIS experiments were implemented in a mixture solution of 0.1 mol L⁻¹ KCl and 1.0 mmol L⁻¹ K₃[Fe(CN)₆]/K₄[Fe(CN)₆] (1:1) with the frequencies changed from 10⁵ to 0.1 Hz.

3. RESULTS AND DISCUSSION

3.1. Characterization of the modified electrodes

Fig. 1 showed the SEM images of different interface of working electrodes. As shown in Fig.1 A, CILE appeared flatly and the void spaces of graphite powders were connected by IL with high viscosity [18]. After electroreduction of GO on CILE surface (Fig. 1B), a 3D porous interface was observed and the GR sheets were connected with each other to form a macrostructure. It can be seen that many porous structures was present on the electrode surface. It had been reported that electrochemical reduction was a common used procedure for the construction of GR modified electrode at simple process and high efficiency [19]. Due to the existence of large quantity of oxygenal groups, GO can be easily reduced to get GR nanosheet under controlled conditions. By using LiClO₄ solution as the electrolyte, the 3D porous macrostructure of GR can be generated on the electrode, which was benefit for the adsorption of biomolecules and acted as effective electronic mediator of enzyme.

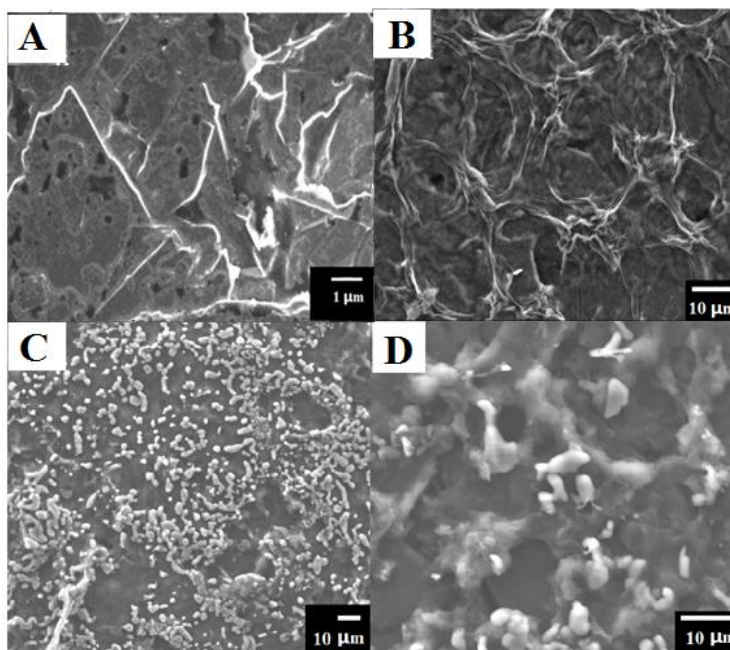


Figure 1. SEM images of (A) CILE, (B) 3DGR/CILE, (C,D) Ag/3DGR/CILE with different magnitude.

Fig. 1 C and D exhibited the SEM results of Ag/3DGR/CILE at different magnitude. Ag nanoparticles were evenly present on the surface of 3D GR with the increase of the active surface area. Electrodeposition has been reported for the fabrication of chemically modified electrodes and Ag nanoparticles could be directly deposited on the electrode surface, which exhibited good performances respective to conductivity, surface area and biocompatibility. Therefore Ag nanoparticles modified electrodes had been reported in electrochemical sensors [20]. Under the selected conditions Ag nanoparticles was electrodeposited on 3DGR to get a Ag/3DGR nanocomposite with the 3D structure remained.

3.2. EIS of the modified electrodes

EIS is often selected to investigate interfacial resistance of the modified electrodes. The presence of various modifiers on the electrode resulted in the change of electron transfer resistance (R_{et}) value correspondingly [21]. EIS experiments were finished in a $1.0 \text{ mmol L}^{-1} [\text{Fe}(\text{CN})_6]^{3-/4-}$ and $0.1 \text{ mol L}^{-1} \text{ KCl}$ mixture solution and the frequencies were scanned from 10^5 to 10^{-1} Hz . Fig. 2 presented the Nyquist diagram of different electrodes and the Randle equivalent circuit (inset of Fig. 2) was selected to check the impedance data. The diameter of the semicircle corresponds to R_{et} value that reflects the interfacial resistance. The R_{et} value of CS/CILE (curve e) was 84.29Ω and that of CS/Ag/3DGR/CILE (curve a) was 13.42Ω , which was due to the presence of high conductive Ag/3DGR nanocomposite with the decrease of the interfacial resistance. On CS/Hb/CILE (curve f) the R_{et} value increased to 107.94Ω , which was due to the existence of Hb on the electrode prevented the electron transfer of $[\text{Fe}(\text{CN})_6]^{3-/4-}$. On CS/Hb/3DGR/CILE (curve d), CS/Hb/Ag/CILE (curve c) and CS/Hb/Ag/3DGR/CILE (curve b), the R_{et} values were gradually decreased to 73.25Ω , 54.17Ω and 38.15Ω , respectively.

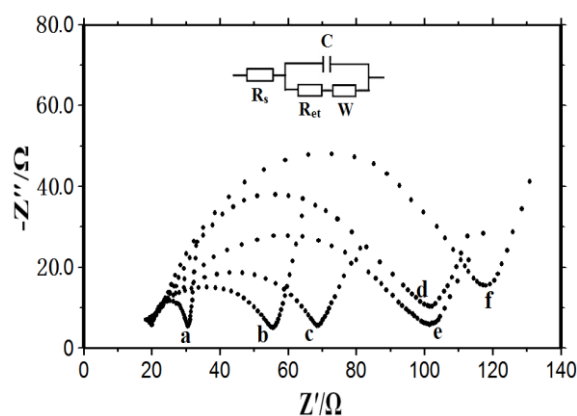


Figure 2. EIS of different electrodes in a $1.0 \text{ mmol L}^{-1} [\text{Fe}(\text{CN})_6]^{3-/4-}$ and $0.1 \text{ mol L}^{-1} \text{ KCl}$ mixture solution with the frequencies from 10^5 to 10^{-1} Hz . Electrodes: (a) CS/Ag/3DGR/CILE, (b) CS/Hb/Ag/3DGR/CILE, (c) CS/Hb/Ag/CILE, (d) CS/Hb/3DGR/CILE, (e) CS/CILE and (f) CS/Hb/CILE.

The decrease of Ret values proved that the increased conductivity of interface with conductive carbon or metal nanoparticles on the electrode surface. Also the Ag/3DGR nanocomposite has the highest conductivity due to the synergistic effects of metal and carbon conductivity, therefore the smallest Ret value appeared. Ag/3DGR nanocomposite has plenty of pores with interconnect structure and large effective area, which facilitates the electron transfer of $[\text{Fe}(\text{CN})_6]^{3-/4-}$ and is beneficial for the electron transfer within the network.

3.3. Direct electrochemical behaviors of the Hb modified electrode

Electrochemical performances of different Hb modified electrodes were checked with cyclic voltammograms shown in Fig. 3. On CS/CILE (curve a), no redox peaks were observed, indicating no electrochemical reaction occurred. On CS/Hb/CILE a pair of unsymmetrical redox waves was observed (curve b), which was ascribed to a slow electron transfer rate between Hb and CILE. CILE has properties including high conductivity, wide electrochemical windows and an IL film on the surface, which can accelerate the electron transfer of redox enzymes/proteins [22]. On CS/Hb/3DGR/CILE (curve c) and CS/Hb/Ag/CILE (curve d) electrochemical responses of Hb were enhanced, which could be attributed to the presence of highly conductive Ag nanoparticle or 3DGR on the electrode surface that was beneficial for fastening the electron transfer rate of Hb. On CS/Hb/Ag/3DGR/CILE (curve e) a couple of well-defined quasi-reversible redox waves appeared with the largest peak currents, indicating that Ag/3DGR nanocomposite was the best mediator for the electron transfer of Hb. 3DGR has high conductivity with many porous structure and Ag nanoparticles are biocompatible metal conductor with large surface area. Therefore the Ag/3DGR nanocomposite could exhibit the synergistic effects to accelerate the electron transfer of Hb.

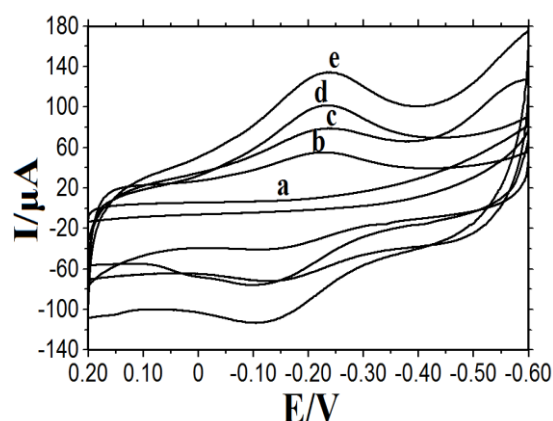


Figure 3. Cyclic voltammograms of (a) CS/CILE, (b) CS/Hb/CILE, (c) CS/Hb/3DGR/CILE, (d) CS/Hb/Ag/CILE and (e) CS/Hb/Ag/3DGR/CILE in pH 3.0 PBS with the scan rate as 100 mV s^{-1} .

From curve e the cathodic peak potential (E_{pc}) of -0.240 V and the anodic peak potential (E_{pa}) of -0.105 V were got, which was resulted from the redox reaction of electroactive center of Hb. The

formal peak potential ($E^{0'}$), which is got from the average value of E_{pc} and E_{pa} , was -0.172 V (vs. SCE) and in agreement to the typical value of the active center of Hb heme Fe(III)/Fe(II) redox couple. Therefore the Ag/3DGR nanocomposites on CILE have the properties such as larger surface-to-volume ratio, faster conductivity and better biocompatibility, which can enhance the absorption amount of proteins and form a best microenvironment for Hb to transfer electrons with electrode.

3.4. Electrochemical investigation

The influence of scan rate (ν) on the cyclic voltammetric curves of CS/Hb/Ag/3DGR/CILE was investigated. As shown in Fig. 4A, a pair of well-defined redox waves was got at various scan rates with almost equal value of redox peak data. The redox peak currents changed linearly with the increase of scan rate from 100 to 1000 mV s^{-1} , indicating a typical thin-layer surface-controlled electrochemical process. Two well-defined linear relationship were got between currents and scan rate with the regression equations as I_{pc} (μA) = 211.31ν (V s^{-1}) + 26.44 ($n = 11, \gamma = 0.993$) and I_{pa} (μA) = -181.86ν (V s^{-1}) - 35.13 ($n = 11, \gamma = 0.992$) (Fig. 4B). By integration of the peak on cyclic voltammograms, the surface coverage (Γ^*) was estimated from the equation ($\Gamma^* = Q/nAF$) [23], where Q is the charge involved in the reaction, n is the number of electrons transferred, F is the Faraday constant, and A is the electrode area. Then the surface coverage (Γ^*) of electroactive Hb was got as 7.9×10^{-10} mol cm^{-2} , which was much larger than that of monolayer coverage (1.89×10^{-11} mol cm^{-2}) [24]. The total amount of Hb casted on the electrode was 1.20×10^{-8} mol cm^{-2} , so the fraction of electroactive Hb from the total Hb was 7.6%. Therefore the porous 3D nanostructure on the electrode was benefit for multilayers Hb to transfer electron with electrode. Ag/3DGR nanocomposite can immobilize more Hb molecules close to the electrode and facilitate the electron transfer from Hb to electrode with fast rate. The increase of scan rate also resulted in the shift of redox peak potentials gradually with the increase of the peak-to-peak separation (ΔE_p), indicating a quasi-reversible electrode process. As shown in Fig. 4C, the relationships of E_p with $\ln \nu$ were linearly with the equations as E_{pc} (V) = $-0.048 \ln \nu - 0.029$ ($n = 7, \gamma = 0.995$) and E_{pa} (V) = $0.039 \ln \nu - 0.076$ ($n = 7, \gamma = 0.994$). According to the Laviron's equations [25]:

$$E_{pc} = E^{0'} - \frac{2.3RT}{\alpha nF} \log \nu \quad (1)$$

$$E_{pa} = E^{0'} + \frac{2.3RT}{(1-\alpha)nF} \log \nu \quad (2)$$

$$\log k_s = \alpha \log(1-\alpha) + (1-\alpha) \log \alpha - \log \frac{RT}{nF\nu} - \frac{(1-\alpha)\alpha F n \Delta E_p}{2.3RT} \quad (3)$$

where ν is the scan rate, n is the electron transfer number, α is the charge transfer coefficient, k_s is the electron transfer rate constant and R , F and T have their common meanings. Based on above equations the values of n , α and k_s were estimated as 0.999, 0.46 and 0.73 s^{-1} . The k_s value can reflect the local microenvironment of the enzymes immobilized on the electrode and this k_s value is located in the range for typical surface-controlled quasi-reversible electrochemical processes. Therefore Ag/3DGR nanocomposite on the electrode could provide a suitable microenvironment for Hb immobilization and undergo facile electron transfer reaction.

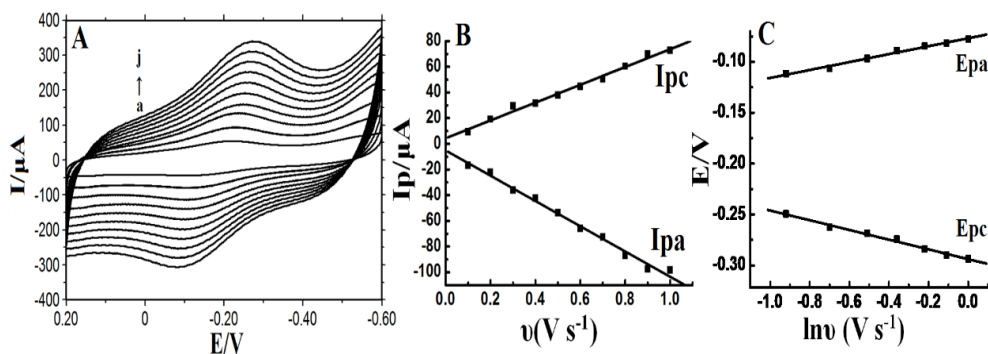


Figure 4. (A) Influence of scan rate on cyclic voltammetric responses of CS/Hb/Ag/3DGR/CILE in pH 3.0 PBS with scan rate from a to j as: 0.1, 0.2, 0.3, 0.4, 0.5, 0.6, 0.7, 0.8, 0.9, 1.0 V s^{-1} . (B) Linear relationship of redox peak current (I_p) versus scan rate (ν). (C) Linear relationship of the redox peak potential versus $\ln \nu$.

3.5. Influence of buffer pH

The effect of buffer pH on cyclic voltammetric responses of CS/Hb/Ag/3DGR/CILE was further investigated in the range from 2.0 to 9.0. As shown in Fig.5A, the electrochemical data were influenced by the buffer pH with the voltammogram changes gradually. The increase of buffer pH resulted in the shift of the redox peak potential negatively, implying the involvement of protons in the electrode reaction.

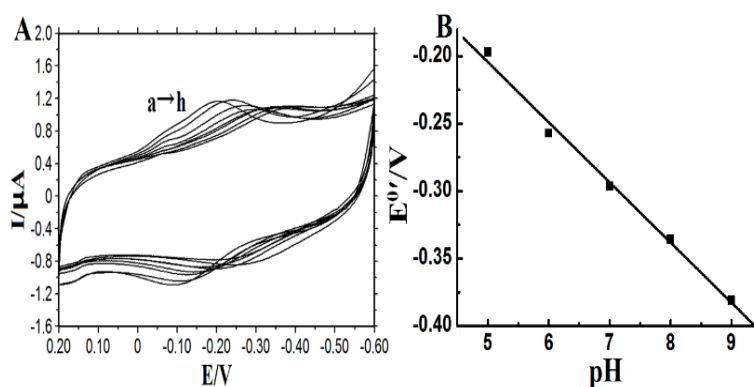


Figure 5. (A) Cyclic voltammograms of CS/Hb/Ag/3DGR/CILE in 0.1 mol L^{-1} PBS at different pH values (from a to h: 2.0, 3.0, 4.0, 5.0, 6.0, 7.0, 8.0, 9.0) with the scan rate as 100 mV s^{-1} ; (B) Linear relationship of the formal peak potential ($E^{0'}$) with pH.

Fig.5B showed the good linear regression relationship of $E^{0'}$ and pH and the equation was $E^{0'} (\text{mV}) = -44.61 \text{ pH} - 18.72$ ($n = 5$, $\gamma = 0.997$). The slope value ($-44.61 \text{ mV pH}^{-1}$) was reasonably a little smaller as compared with the theoretical value (-59 mV pH^{-1}). The reason may be due to the effects of the protonation states of transligands to the heme iron, and amino acids around the heme to the protonation of water molecules coordinated to the center that may be present in different states at

different pH [26]. Therefore, the electron transfer reaction of Hb and the electrode can be presented as: Hb heme Fe (III) + H⁺ + e⁻ ↔ Hb heme Fe (II). The largest peak current was observed at pH 3.0 solution, which could provide enough protons for electrochemical reaction and was selected for all the electrochemical experiment.

3.6. Stability and reproducibility of Hb modified electrode

The stability of CS/Hb/Ag/3DGR/CILE was evaluated by examining the cyclic voltammetric responses of the modified electrode with continuous scanning in pH 3.0 PBS. 97.6% of the initial response was kept after 50 cycles and 89.7% after scanning 500 cycles, indicating good stability of CS/Hb/Ag/3DGR/CILE in PBS. Seven electrodes were fabricated and used to check the reproducibility by cyclic voltammetry with the relative standard deviation (RSD) as 2.5%. So Hb molecules on the electrode maintained its electroactivity with good stability and reproducibility, which was due to specific properties of Ag/3DGR nanocomposite that could remain the biological activity of Hb.

4. CONCLUSIONS

In this paper Ag nanoparticle and 3DGR nanocomposite were electrodeposited on CILE and the fabricated Ag/3DGR/CILE exhibited good biocompatibility and high conductivity, which could be further acted as the basic electrode for Hb immobilization to construct a protein modified electrode (CS/Hb/Ag/3DGR/CILE). Due to the high conductivity of Ag/3DGR nanocomposite with network structure, direct electrochemistry of Hb was accelerated with a couple of well-defined quasi-reversible redox peaks observed. A comparison of the electrochemical parameters of this Hb modified electrode with other reported Hb electrodes was listed in table 1. The prepared CS/Hb/Ag/3DGR/CILE showed good stability and reproducibility, which had the potential application in the electrochemical sensor. Therefore electrodeposition of Ag/3DGR nanocomposite is a simple and efficient procedure for the preparation nanomaterials modified electrode with high activity.

Table 1. Comparison of electrochemical parameters of Hb based electrochemical sensors

Electrode	E ⁰ /V	Γ*/mol cm ⁻¹	α	k _s /s ⁻¹	[refs]
Nafion/Hb/Au/CILE	-0.210	2.62×10 ⁻⁹	0.573	0.412	27
CTS/Hb-Fe ₃ O ₄ /CILE	-0.287	9.75×10 ⁻⁹	0.29	0.478	28
Nafion/GR-TiO ₂ -Hb/CILE	-0.216	1.1×10 ⁻⁹	0.48	0.65	29
CTS/GR-LDH-Hb/CILE	-0.196	8.4×10 ⁻¹⁰	0.56	0.64	30
CTS/Cu ₃ Mo ₂ O ₉ -Hb/CILE	-0.196	1.42×10 ⁻⁹	0.7	0.608	31
Hb/Au-cysteamine/AuE	-0.051	6.71×10 ⁻¹¹	0.5	0.49	32
CS/Hb/Ag/3DGR/CILE	-0.172	7.9×10 ⁻¹⁰	0.46	0.73	This work

ACKNOWLEDGEMENTS

We acknowledge the financial support from the Beijing Natural Science Foundation (7142006).

References

1. C. Léger and P. Bertrand, *Chem. Rev.*, 108 (2008) 2379
2. F. A. Armstrong and G. S. Wilson, *Electrochim. Acta*, 45 (2000) 2623
3. J. F. Rusling, *Acc. Chem. Res.*, 31 (1998) 363
4. F. Shi, W. Z. Zheng, W. C. Wang, F. Hou, B. X. Lei, Z. F. Sun and W. Sun, *Biosens. Bioelectron.*, 64 (2015) 131
5. T. R. Zhan, Y. Q. Guo, L. Xu, W. L. Zhang, W. Sun and W.G. Hou, *Talanta*, 94 (2012) 189
6. E. J. Parker-Williams, *Medicine*, 37 (2009) 137
7. H. Y. Zhao, W. Zheng, Z. X. Meng, H. M. Zhou, X. X. Xu, Z. Li and Y. F. Zheng, *Biosens. Bioelectron.*, 24 (2009) 2352
8. F. Shi, W. C. Wang, S. X. Gong, B. X. Lei, G. J. Li, X. M. Lin, Z. F. Sun and W. Sun, *J. Chin. Chem. Soc.*, 62 (2015) 554
9. S. S. Jia, J. J. Fei, J. P. Zhou, X. M. Chen and J. Q. Meng, *Biosens. Bioelectron.*, 24 (2009) 3049
10. Y. Zhang, X. M. Sun and N. Q. Jia, *Sens. Actuators B*, 157 (2011) 527
11. F. Arduini, S. Cinti, V. Scognamiglio and D. Moscone, *Microchim. Acta*, 183 (2016) 1
12. C. M. Welch, C. E. Banks, A. O. Simm and R. G. Compton., *Anal. Bioanal. Chem.*, 382 (2005) 12
13. J. Liu, Z. Liu, C. J. Barrow and W. Yang, *Anal. Chim. Acta*, 859 (2015) 1
14. Q. Fang, Y. Shen and B. Chen, *Chem. Eng. J.*, 264 (2015) 753
15. W. Sun, F. Hou, S. X. Gong, L. Han, W. C. Wang, F. Shi, J. W. Xi, X. L. Wang and G. J. Li, *Sens. Actuators B*, 219 (2015) 331
16. W. Sun, M. X. Yang and K. Jiao, *Anal. Bioanal. Chem.*, 389 (2007) 1283
17. C. Li and G. Q. Shi, *Nanoscale*, 4 (2012) 5549
18. W. Sun, Y. Y. Zhang, X. Z. Wang, X. M. Ju, D. Wang, J. Wu and Z. F. Sun, *Electroanalysis*, 24 (2012) 1973
19. M. Zhou, Y. L. Wang, Y. M. Zhai, J. F. Zhai, W. Ren and F. A. Wang, *Chem Eur J.*, 15 (2009) 6116
20. C. M. Yu, X. H. Zhou, H. Y. Gu, *Electrochim. Acta*, 55 (2010) 8738
21. S. Palanisamy, C. Karuppiah, S. M. Chen, *Colloids Surf. B*, 114 (2014) 164
22. W. Sun, D. D. Wang, R. F. Gao and K. Jiao, *Electrochem. Commun.*, 9 (2007) 1159
23. A. J. Bard and L. R. Faulkner, *Electrochemical Methods*. Wiley, New York 1980
24. S. F. Wang, T. Chen, Z. L. Zhang, X. C. Shen, Z. X. Lu, D. W. Pang and K. Y. Wong, *Langmuir*, 21 (2005) 9260
25. E. Laviron, *J. Electroanal. Chem.*, 101 (1979) 19
26. I. Yamazaki, T. Araiso, Y. Hayashi, H. Yamada and R. Makino, *Adv. Biophys.*, 11 (1978) 249
27. W. Sun, P. Qin, R. J. Zhao and K. Jiao, *Talanta*, 80 (2010) 2177
28. W. Sun, Z. L. Sun, L. Q. Zhang and X. W. Qi, *Colloids Surf. B*, 101 (2013) 177
29. W. Sun, Y. Q. Guo, X. M. Ju and Y. Y. Zhang, *Biosens. Bioelectron.*, 42 (2013) 207
30. W. Sun, Y. Q. Guo, Y. P. Lu and A. H. Hu, *Electrochim. Acta*, 91 (2013) 130
31. L. Q. Zhang, T. T. Li, Y. Deng and Y. Y. Zhang, *J. Iran. Chem. Soc.*, 11 (2014) 407
32. H. Y. Gu, A. M. Yu, H. Y. Chen, *J. Electroanal. Chem.* 516 (2001) 119